Inorganic Chemistry

Article

pubs.acs.org/IC

Three New Sodium Neptunyl(V) Selenate Hydrates: Structures, Raman Spectroscopy, and Magnetism

Geng Bang Jin,* S. Skanthakumar, and L. Soderholm

Chemical Sciences and Engineering Division, Argonne National Laboratory, Argonne, Illinois 60439, United States

Supporting Information

ABSTRACT: Green crystals of $Na(NpO_2)(SeO_4)(H_2O)$ (**1**), $Na_3(NpO_2)(SeO_4)_2(H_2O)$ (**2**), and $Na_3(NpO_2)(SeO_4)_2(H_2O)_2$ (**3**) have been prepared by a hydrothermal method for **1** or evaporation from aqueous solutions for **2** and **3**. The structures of these compounds have been characterized by single-crystal X-ray diffraction. Compound **1** is isostructural with $Na(NpO_2)(SO_4)(H_2O)$ (**4**). The structure of **1** consists of ribbons of neptunyl(V) pentagonal bipyramids, which are decorated and further connected by selenate tetrahedra to form a three-dimensional framework. The resulting open channels are filled by Na^+ cations and H_2O molecules. Within the ribbon, each neptunyl polyhedron shares corners with each other solely through cation−cation interactions (CCIs). The structure of **2** adopts one-dimensional $[(NpO_2)(SeO_4)_2(H_2O)]^{3-}$ chains connected by Na^+ cations. Each NpO_2^+ cation is coordinated by four monodentate SeO_4^{2-} anions and one H_2O molecule to form a pentagonal bipyramid. The structure of **3** is constructed by one-dimensional $[(NpO_2)(SeO_4)_2]^{3-}$ chains separated by Na^+ cations and H_2O molecules. These chains have two configurations resulting in two disordered orientations of the $Se(2)O_4^{2-}$ tetrahedra. Each NpO_2^+ cation is coordinated by one bidentate $Se(1)O_4^{2-}$ and three monodentate $Se(2)O_4^{2-}$ anions to form a pentagonal bipyramid. Raman spectra of **1**, **2**, and **4** were collected on powder samples. For **1** and **4**, the neptunyl symmetric stretch modes (670, 676, 730, and 739 cm^{-1}) shift significantly toward lower frequencies compared to that in **2** (773 cm^{-1}), and there are several asymmetric neptunyl stretch bands in the region of 760−820 cm^{-1}. Magnetic measurements obtained from crushed crystals of **1** are consistent with a ferromagnetic ordering of the neptunyl(V) spins at 6.5(2) K, with an average low temperature saturation moment of 2.2(1) μ_B per Np. Well above the ordering temperature, the susceptibility follows Curie−Weiss behavior, with an average effective moment of 3.65(10) μ_B per Np and a Weiss constant of 14(1) K. Correlations between lattice dimensionality and magnetic behavior are discussed.

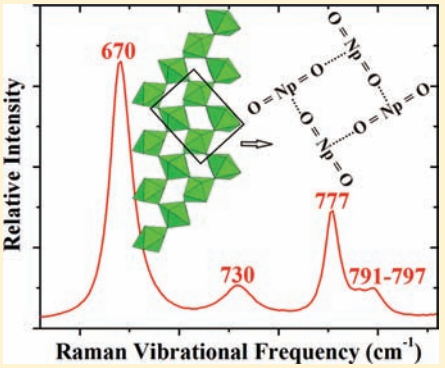

INTRODUCTION

Much of neptunium (Np) chemistry lies between that of uranium (U) and plutonium (Pu) in the actinide series, as evidenced by their relative reduction potentials.[1] The impact is clearly seen in aqueous solution, where U^{6+}, Np^{5+}, and Pu^{4+} predominate under most conditions. The former two exist almost exclusively as linear dixoxo moieties, which can be further coordinated by four to six ligands in the equatorial plane.[2−5] Usual to the neptunyl(V) ion, NpO_2^+, is its tendency to bond to other NpO_2^+ units as an equatorial ligand, a configuration referred to as a cation−cation interaction (CCI).[5,6] First reported for neptunyl(V) ions in acidic solution,[7] a large proportion of the NpO_2^+ compounds for which structures have been reported exhibit these interactions.[6] Each NpO_2^+ cation can act both as a coordinating center and a ligand and participates in one to four or six CCIs in total.[6,8] Recently we reported a new neptunyl(V) selenite, $(NpO_2)_3(OH)(SeO_3)(H_2O)_2{\cdot}H_2O$, with a novel CCI framework, within which one of NpO_2^+ cations is involved with five CCIs.[9] As a result of this unusual bonding interaction, neptunyl(V) compounds exhibit diverse metal−ion lattice connectivities ranging from zero-dimensional NpO_2^+ dimers, one-dimensional chains, ribbons, two-dimensional sheets, to condensed three-dimensional structures. In addition, the IR spectra of neptunyl(V) compounds with CCIs have noticeable shifts of the asymmetric stretch bands toward lower frequencies due to changes in the strength of the Np−O interaction.[10,11] To the best of our knowledge, all neptunyl(V) compounds reported to exhibit magnetic ordering include CCIs.[12] This may be in part owing to potential superexchange pathways provided by CCIs that can enhance magnetic interactions between Np(V) ($5f^2$) ions.[13] The Np−Np ion connectivity is enhanced by CCIs, often with resulting fractal lattice dimensionality that can be used as a tool for systematic probing the subtle relationship between lattice and spin dimensionality and magnetic behavior.

To further explore the role of CCIs on the crystal chemistry, vibrational energies, and magnetic properties of neptunyl(V) compounds, we focus on the neptunyl(V) selenate system, where the structurally flexible SeO_4^{2-} ligand can potentially stabilize various CCI networks.[14] We started with a

Received: December 15, 2011
Published: February 22, 2012

   dx.doi.org/10.1021/ic202703j | *Inorg. Chem.* 2012, 51, 3220−3230

reinvestigation of three neptunyl(V) selenate hydrates, $(NpO_2)_2(SeO_4)(H_2O)_n$ (n = 1, 2, and 4).[12] In the absence of other cations in solution during synthesis, the neptunyl(V) oxo groups appear to utilize neighboring NpO_2^+ units to complete their bonding requirements, thus forming CCIs. Our single-crystal structural studies confirmed the presence of similar CCI lattices for all three selenates as those in related sulfates and the tetrahydrate was found to undergo a ferromagnetic transition below 8(1) K.[12] Interestingly, the local coordination environment and geometry around one of the NpO_2^+ cations in the selenate monohydrate deviates from those in the sulfate analogue. This effect results from different interactions between the neptunyl unit and ligands. The divergence in the NpO_2^+−sulfate and −selenate interactions is consistent with the high energy X-ray scattering (HEXS) studies on UO_2^{2+}−sulfate and selenate ion pairs in aqueous solutions.[15−17]

Continuing our effort to explore the neptunyl(V) selenates, we present the syntheses and single-crystal structures of three new sodium neptunyl(V) hydrates: $Na(NpO_2)(SeO_4)(H_2O)$ (**1**), $Na_3(NpO_2)(SeO_4)_2(H_2O)$ (**2**), and $Na_3(NpO_2)(SeO_4)_2(H_2O)_2$ (**3**). Compound **1** contains CCIs, while compounds **2** and **3** do not. The effect of Na^+ cations and H_2O on the neptunyl(V) lattice dimensionality are discussed, together with structural differences between these selenates and their sulfate analogues. Raman spectra of compound **1** and **2** together with the magnetic susceptibility of **1** as a function of temperature provide input into the Np−Np electronic connectivity and its change with lattice dimensionality via varying CCIs. The Raman spectrum of $Na(NpO_2)(SO_4)(H_2O)$ (**4**),[18] which is isostructural with **1**, is also included in the discussion. Raman spectrometry has been previously used to identify and measure the formation of neptunyl(V) complexes in the aqueous solutions; however, studies on solid neptunyl(V) phases are very scarce.[19−21] To our knowledge, these are the first reported Raman spectra for solid-state neptunyl(V) compounds with CCIs.

EXPERIMENTAL SECTION

Caution! *^{237}Np is α- and γ-emitting radioisotope and as such is considered a health risk. Its use requires appropriate infrastructure and personnel trained in the handling of radioactive materials.*

Hydrothemal Synthesis of $Na(NpO_2)(SeO_4)(H_2O)$ (1). A 0.150 mL portion of a 0.167 M Np(V) stock solution (in ∼0.87 M HCl), 111.8 mg (0.303 mmol) of $Na_2SeO_4{\cdot}10H_2O$ (Aldrich, 99.999%), and 0.065 mL of a 2 M NaOH (Fisher, 98.5%) solution were added to a 3 mL Teflon cup with a tightly closed screw-top lid. The pH of resulting solution was estimated to be about 3. Two such Teflon cups were placed in a 125 mL Teflon-lined Parr reaction vessel with 30 mL counter-pressure water and heated in a convection oven at 150 °C for 6 days, then the oven was turned off. Large green prisms of **1** were the only solid product found, and the yield of **1** based on Np is close to 100%, estimated by inspection and from analyses of powder X-ray diffraction data.

Syntheses of $Na_3(NpO_2)(SeO_4)_2(H_2O)$ (2) and $Na_3(NpO_2)(SeO_4)_2(H_2O)_2$ (3). The reaction mixture of **2** was the same as that of **1** and was loaded to a 3 mL Teflon cup as well. For the reaction of **3**, the reactants included 0.215 mL of a 0.116 M Np(V) stock solution (in ∼1 M HCl), 106.0 mg (0.287 mmol) of $Na_2SeO_4{\cdot}10H_2O$ (Aldrich, 99.999%), and 0.785 mL of distilled H_2O, which were added to a 7 mL Teflon cup. The pH of resulting solution for **3** was adjusted to 3.47 using a 2 M NaOH (Fisher, 98.5%) solution. Both Teflon cups were left open inside of a fume hood allowing evaporation of most of water, and then were closed tightly with a screw-top lid. After several months, the solution for **2** reached a near dryness with numerous colorless crystals of Na_2SeO_4,[22] a green aggregate, and a large number of small green crystals of **2**. The yield of **2** is about 10% based on Np from a visual inspection. The solution for **3** was completely dry resulting in a green aggregate and a large number of green prisms of **3** covered by a white salt. The yield of **3** is about 20% based on Np from a visual inspection.

Hydrothemal Synthesis of $Na(NpO_2)(SO_4)(H_2O)$ (**4**) has been described.[18]

Structure Determinations. Single-crystal X-ray diffraction data for $Na(NpO_2)(SeO_4)(H_2O)$ (**1**), $Na_3(NpO_2)(SeO_4)_2(H_2O)$ (**2**), and $Na_3(NpO_2)(SeO_4)_2(H_2O)_2$ (**3**) were collected with the use of graphite-monochromatized Mo Kα radiation (λ = 0.71073 Å) at 100 K on a Bruker APEX2 diffractometer.[23] The crystal-to-detector distance was 5.106 cm. Data were collected by a scan of 0.3° in ω in groups of 600 frames at φ settings of 0°, 90°, 180°, and 270°. The exposure time was 30 s/frame for **1**, 40 s/frame for **2**, and 20 s/frame for **3**. The collection of intensity data as well as cell refinement and data reduction were carried out with the use of the program APEX2.[23] Absorption corrections as well as incident beam and decay corrections were performed with the use of the program SADABS.[24] The structures were solved with the direct-methods program SHELXS and refined with the least-squares program SHELXL.[25]

During the structural refinements of **1**, large displacement parameters were found for the Na(3) position, absent an indication of sites splitting in the difference Fourier map. The occupancy refinement suggested that the Na(3) site is fully occupied. Attempts to model the disordering of Na atoms into the Na(3) position and the nearest Q peak failed. The Na(3) atom was finally refined in one ordered position with a large thermal ellipsoid elongated along the [001] direction. The refinement of the structure of **2** was straightforward. In the case of **3**, large displacement parameters were found for Na(1), O(3), and O(4) atoms. Residue electron densities located in difference Fourier maps near Na(1) and O(3), and a short distance (∼0.8 Å) between neighboring O(4) positions indicating all three sites are disordered. We refined the disordering of O(3) and O(4) atoms first. As such, O(3) was split over two positions, O(3) and O(3A). The occupancies of the O(3), O(3A), and O(4) site were refined to be sufficiently close to 50%, and then, they were constrained to be 0.5 before further refinements. Attempts to model the disordering of Na(1) atoms over two positions and refine their occupancies with a constrained total value of 0.5 and anisotropic displacement parameters resulted in nonpositive displacement ellipsoids for Na(1) and Na(1A) atoms. Finally, the corresponding refinements with isotropic displacement parameters were carried out and the occupancies of Na(1) and Na(1A) atoms were determined to be 0.29(1) and 0.21(1), respectively.

For all three structures, the H atoms of the water molecules were found in the difference maps. H positions were refined using O−H and H−H distance constraints of 0.83 and 1.40 Å, respectively. Each final refinement included anisotropic displacement parameters for all non-hydrogen atoms except Na(1) and Na(1A) atoms in **3**. The program STRUCTURE TIDY[26] was used to standardize the positional parameters. Additional experimental details are given in Table 1 and in the Supporting Information.

Powder X-ray Diffraction Measurements. Powder X-ray diffraction patterns were collected with a Scintag X1 diffractometer with the use of Cu Kα radiation (λ = 1.5418 Å). The powder sample was loaded into an encapsulated container with curved Kapton windows to minimize the X-ray absorption by the Kapton.

Raman Spectroscopy. Raman spectra of powder samples of $Na(NpO_2)(SeO_4)(H_2O)$ (**1**), $Na_3(NpO_2)(SeO_4)_2(H_2O)$ (**2**), and $Na(NpO_2)(SO_4)(H_2O)$[18] (**4**) were collected on a Renishaw inVia Raman Microscope with an excitation line of 532 nm. Due to the radiological hazards associated with ^{237}Np, each sample was placed on a glass drop-slide covered with a transparent coverslip, which was sealed to the slide using an epoxy sealant.

Magnetic Susceptibility Measurements. A superconducting quantum interference device (SQUID) magnetometer was used to measure the magnetic response of two crushed, single-crystal samples of $Na(NpO_2)(SeO_4)(H_2O)$ (**1**), weighing a total of 8.2 and 3.6 mg respectively, over the temperature range of 2−320 K. Due to the radiological hazards associated with ^{237}Np, the sample was double-

dx.doi.org/10.1021/ic202703j | Inorg. Chem. 2012, 51, 3220−3230

Table 1. Crystal Data and Structure Refinements for $Na(NpO_2)(SeO_4)(H_2O)$ (1), $Na_3(NpO_2)(SeO_4)_2(H_2O)$ (2), and $Na_3(NpO_2)(SeO_4)_2(H_2O)_2$ (3)[a]

	$Na(NpO_2)(SeO_4)(H_2O)$	$Na_3(NpO_2)(SeO_4)_2(H_2O)$	$Na_3(NpO_2)(SeO_4)_2(H_2O)_2$
F_w	452.97	641.91	659.92
color and habit	green plate	green prism	green prism
crystal system	monoclinic	triclinic	monoclinic
space group	$C2/c$	$P\bar{1}$	$P2_1/m$
Z	16	2	2
a (Å)	18.661(3)	6.974(1)	7.8061(7)
b (Å)	5.6987(8)	7.983(1)	7.1101(6)
c (Å)	24.167(3)	9.690(2)	11.0967(9)
α (deg)		90.113(3)	
β (deg)	102.999(2)	95.914(3)	91.159(1)
γ (deg)		112.149(2)	
V (Å^3)	2504.2(6)	496.6(2)	615.76(9)
ρ_c (g/cm^3)	4.806	4.293	3.559
μ (cm^{-1})	224.62	179.74	145.06
$R(F)^b$	0.0304	0.0288	0.0282
$R_w(F_o^2)^c$	0.0695	0.0596	0.0698

[a]For all structures, $\lambda = 0.71073$ Å and $T = 100(2)$ K. [b]$R(F) = \sum||F_o| - |F_c||/\sum|F_o|$ for $F_o^2 > 2\sigma(F_o^2)$. [c]$R_w(F_o^2) = \{\sum[w(F_o^2 - F_c^2)^2]/\Sigma wF_o^4\}^{1/2}$.

encapsulated in a sealed aluminum holder that contributed considerably (up to 80−90% at high temperatures) to the measured response. Low temperature hysteresis measurements were obtained at 2, 5, 10, 15, 20, 30, and 300 K as a function of field to a maximum of 4 T. Magnetization data as a function of temperature were acquired under applied fields of 0.0025, 0.005, 0.01, 0.05, 0.2, and 0.5 T. Empty Al sample holders were measured separately under identical conditions, and their magnetic response was subtracted directly from the raw data. The measured susceptibility data was further corrected by removing the Langevin diamagnetic contribution of the sample from the raw data.[27,28] Insufficient quantities of the other two new materials, $Na_3(NpO_2)(SeO_4)_2(H_2O)$ (2) and $Na_3(NpO_2)(SeO_4)_2(H_2O)_2$ (3) were available to characterize their magnetic responses.

RESULTS

Syntheses. Compound 1 was prepared through a hydrothermal reaction in almost 100% yield, while compounds 2 and 3 were prepared under ambient conditions in much lower yields, and they were difficult to separate from other products.

During the course of exploring the neptunyl(V) selenate system, numerous reactions were conducted in order to investigate the effects of reactant compositions, solution pH, and the heating conditions on the final products. For example, an excess of Na_2SeO_4 in the starting materials resulted in Na incorporation into the neptunyl product as demonstrated by the titled syntheses compared to those for $(NpO_2)_2(SeO_4)(H_2O)_n$ (n = 1, 2, 4).[12] All neptunyl(V) selenates were prepared under acidic conditions, which is not surprising since neptunyl(V) ions will be considerably hydrolyzed when the solution pH is above 7.[3] This is also true for the syntheses of neptunyl(V) sulfates.[18,29−31] The reactant compositions for the syntheses of 1 with CCIs and 2 without CCIs (see below) are identical, but they were heated differently. This suggests that hydrothermal treatment may help to stabilize CCI complexes in 1.

Structures. $Na(NpO_2)(SeO_4)(H_2O)$ (1) is isostructural to $Na(NpO_2)(SO_4)(H_2O)$ (4).[18] As shown in Figure 1a, the structure of 1 adopts a three-dimensional framework of

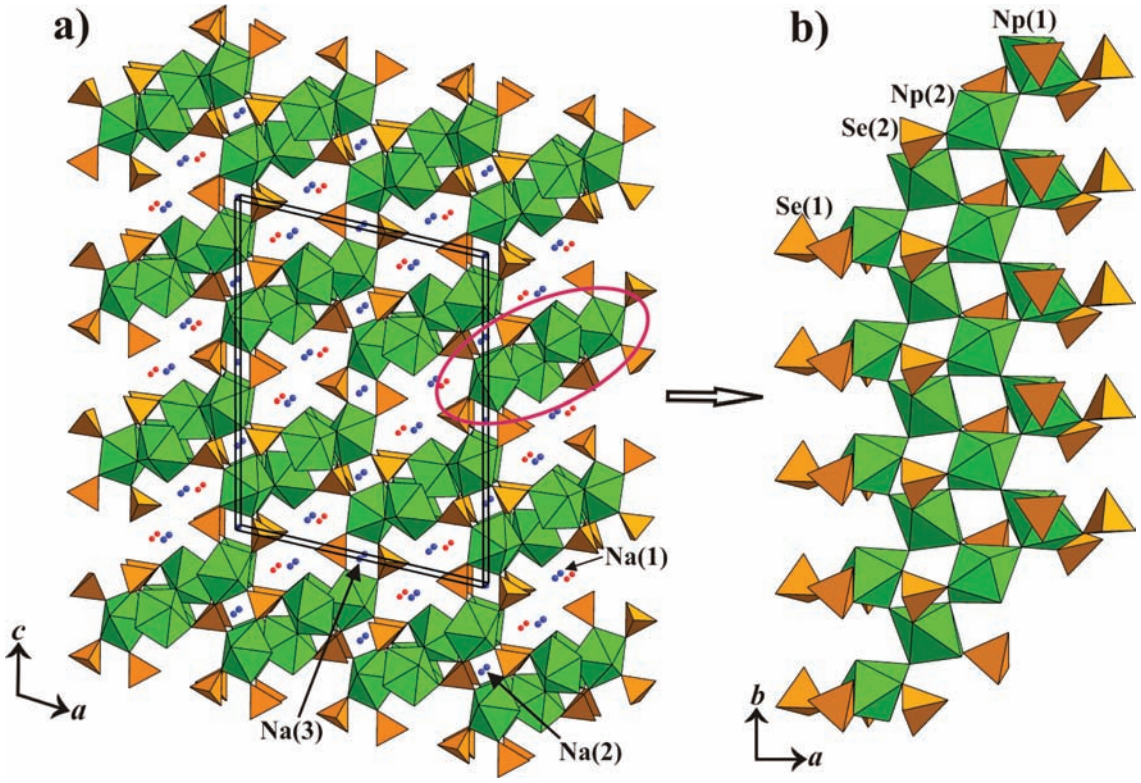

Figure 1. (a) Three-dimensional structure of $Na(NpO_2)(SeO_4)(H_2O)$ (1) constructed by neptunyl(V) selenate ribbons (circled in red) with open channels along the [010] direction filled by Na^+ cations (blue balls) and H_2O molecules (red balls). (b) Depiction of an individual ribbon of corner-sharing green NpO_7 pentagonal bipyramids decorated by orange SeO_4 tetrahedra.

dx.doi.org/10.1021/ic202703j | Inorg. Chem. 2012, 51, 3220−3230

neptunyl(V) selenates with three different sized open channels along the [010] direction, which are filled by Na^+ counter cations. Within the neptunyl selenate network, each neptunyl polyhedron corner shares with other units to form ribbons (Figure 1b), which are further connected by selenate tetrahedra via vertices. There are two crystallographically unique Np, two Se, and three Na positions (site symmetry of 2 for Na(2) and site symmetry of $\bar{1}$ for Na(3)). Each Np atom is bonded to two O atoms in a nearly linear fashion to form a NpO_2^+ cation, which is further coordinated by five ligands in the equatorial plane in a pentagonal bipyramidal geometry. Each $Np(1)O_2^+$ cation is coordinated by one $Np(2)O_2^+$ unit, two monodentate $Se(1)O_4^{2-}$ and two monodentate $Se(2)O_4^{2-}$ anions, while each $Np(2)O_2^+$ cation is coordinated by one $Np(1)O_2^+$ and one $Np(2)O_2^+$ unit, two monodentate $Se(2)O_4^{2-}$ anions, and one $H_2O(8)$ molecule. The Np−O distances within the NpO_2^+ unit range from 1.825(4) to 1.857(4) Å, and O−Np−O angles are 176.1(2) and 178.4(2)° (Table 2). The equatorial Np−O distances range from 2.427(4) to 2.532(4) Å. Each $Se(1)O_4^{2-}$ tetrahedron is bound to two $Np(1)O_2^+$ cations, and each $Se(2)O_4^{2-}$ tetrahedron is bound to two $Np(1)O_2^+$ and two $Np(2)O_2^+$ cations. Se−O distances within selenate groups are in the range of 1.621(4) and 1.649(4) Å. The $Na(3)^+$ cation has a large displacement parameters along the [001] direction, which has been observed in the structure of **4** as well.[18] Each $Na(1)^+$, $Na(2)^+$, and $Na(3)^+$ cation is surrounded by six, eight, and six O atoms, respectively, from the $Np(1)O_2^+$, SeO_4^{2-}, and H_2O units, respectively. Na−O distances are in the range of 2.264(5) and 3.030(5) Å. Each $H_2O(8)$ molecule binds to one $Np(2)O_2^+$ cation in the equatorial plane and connects to Na^+ cations, while $H_2O(14)$ only connects to Na cations. Hydrogen bonding interactions involving water molecules are present in compound **1** and compounds **2** and **3** as well, which will not be discussed in detail here.

Table 2. Selected Interatomic Distances (Å) and Angles (deg) for $Na(NpO_2)(SeO_4)(H_2O)$ (1)

Np(1)−O(1)	1.825(4)	Se(1)−O(2)	1.643(4)
Np(1)−O(11)	1.857(4)	Se(1)−O(4)	1.639(4)
Np(1)−O(2)	2.462(4)	Se(1)−O(6)	1.621(4)
Np(1)−O(3)	2.454(4)	Se(1)−O(12)	1.649(4)
Np(1)−O(5)	2.461(4)	Se(2)−O(3)	1.643(4)
Np(1)−O(12)	2.460(4)	Se(2)−O(9)	1.632(4)
Np(1)−O(13)	2.469(4)	Se(2)−O(10)	1.636(4)
Np(2)−O(5)	1.840(4)	Se(2)−O(13)	1.628(4)
Np(2)−O(7)	1.854(4)	Np(1)−Np(2)[a]	4.0644(5)
Np(2)−O(7)	2.453(4)	Np(1)−Np(2)[a]	4.1409(5)
Np(2)−O(8)	2.532(4)	Np(2)−Np(2)[a] × 2	4.1815(5)
Np(2)−O(9)	2.489(4)	Np(1)−Np(1)[b]	5.9547(8)
Np(2)−O(10)	2.427(4)	Np(1)−Np(1)[b]	6.486(1)
Np(2)−O(11)	2.435(4)	O(1)−Np(1)−O(11)	176.1(2)
		O(5)−Np(2)−O(7)	178.4(2)

[a]Within a single neptunyl ribbon. [b]Between adjacent neptunyl ribbons.

The neptunyl cations within the ribbon of **1** are connected to each other through CCIs. Each $Np(1)O_2^+$ cation acts as a center coordinated by one $Np(2)O_2^+$ unit and also as a ligand binds to one $Np(2)O_2^+$ center, while each $Np(2)O_2^+$ cation acts as a center coordinated by one $Np(1)O_2^+$ and one $Np(2)O_2^+$ unit and also as a ligand binds to one $Np(1)O_2^+$ and one $Np(2)O_2^+$ center. Therefore each $Np(1)O_2^+$ and $Np(2)O_2^+$ cation participates in two and four CCIs, respectively. The Np−Np distances corresponding to CCIs range from 4.0644(5) to 4.1815(5) Å, which are comparable to other reported Np(V)−Np(V) distances corresponding to CCIs.[6] The closest Np−Np distances among adjacent ribbons, bridged by two selenate groups, are 5.9547(8) and 6.486(1) Å.

$Na_3(NpO_2)(SeO_4)_2(H_2O)$ (**2**) crystallizes in the triclinic space group $P\bar{1}$. As shown in Figure 2, the structure of **2** consists of $[(NpO_2)(SeO_4)_2(H_2O)]^{3-}$ chains along the $[0\bar{1}1]$ direction, which are separated by Na^+ cations. A single neptunyl selenate polyhedral chain is shown in Figure 2b, within which neptunyl pentagonal bipyramids are bridged by two monodentate selenate tetrahedra down the chain propagation direction. The topology of $[(NpO_2)(SeO_4)_2(H_2O)]^{3-}$ chains have not been observed in neptunyl(V) sulfates; however, it is common for uranyl(VI) compounds with tetrahedral TO_4^{n-} (T = S, Se, P, As) anions, such as $Mn[(UO_2)(SO_4)_2(H_2O)](H_2O)_4$ and $M[(UO_2)(SeO_4)_2(H_2O)](H_2O)_4$ (M = Mg, Zn).[32−35] There are one crystallographically unique Np, two Se, and three Na positions in **2**. The Np atom is bonded to two O atoms in a nearly linear fashion to form a NpO_2^+ cation, which is further coordinated by four monodentate SeO_4^{2-} anions and one $H_2O(7)$ molecule in the equatorial plane in a pentagonal bipyramidal geometry. The Np−O distances within the NpO_2^+ unit are 1.813(3) and 1.831(3) Å, and the O−Np−O angle is 176.4(2)° (Table 3). The equatorial Np−O distances range from 2.445(3) to 2.576(3) Å, with Np−O(7) being the longest. The Np−Np distances between two neighboring NpO_2^+ units within $[(NpO_2)(SeO_4)_2(H_2O)]^{3-}$ chains are 6.2541(9) and 6.5202(9) Å, while the closest Np−Np distances between adjacent chains are 6.3440(9) and 6.4090(8) Å. Each SeO_4^{2-} tetrahedron connects two NpO_2^+ cations with Se−O distances ranging from 1.621(3) and 1.653(3) Å. The interstitial Na^+ cation is surrounded by seven O atoms for Na(1), six for Na(2), and seven for Na(3), respectively, from NpO_2^+, SeO_4^{2-}, and H_2O units. Na−O distances are in the range of 2.274(4) and 2.928(4) Å.

$Na_3(NpO_2)(SeO_4)_2(H_2O)_2$ (**3**) crystallizes in the monoclinic space group $P2_1/m$. The structure of **3** contains $[(NpO_2)(SeO_4)_2]^{3-}$ chains along the [010] direction, which are connected by Na^+ cations and H_2O molecules (Figure 3a). Neptunyl selenate polyhedral chains are constructed by edge and corner sharing NpO_7 pentagonal bipyramids and SeO_4 tetrahedra (Figure 3b). There are one crystallographically independent Np, two Se, four Na, and ten O positions. Atoms Np(1), Se(1), Se(2), Na(2), and O(6)−O(9) have site symmetry m, Na(3) has site symmetry $\bar{1}$, and the rest of atoms are in general positions. As discussed above, O(3) and O(4) atoms from $Se(2)O_4^{2-}$ anions disorder over two positions with half occupancy each, as depicted in Figure 3b. This is due to the existence of two configurations of $[(NpO_2)(SeO_4)_2]^{3-}$ chains that are related by symmetry operation 2_1 (Figure 3c). The Np atom is bonded to two O atoms in a nearly linear fashion to form a NpO_2^+ cation, which is further coordinated by one bidentate $Se(1)O_4^{2-}$ and three monodentate $Se(2)O_4^{2-}$ anions in the equatorial plane in a pentagonal bipyramidal geometry. The Np−O distances within the NpO_2^+ unit are 1.838(7) and 1.815(7) Å, and the O−Np−O angle is 179.8(3)°. The equatorial Np−O distances range from 2.38(1) to 2.547(5) Å (Table 4). The Np−Np distances between two neighboring NpO_2^+ units within $[(NpO_2)(SeO_4)_2]^{3-}$ chains are 5.9605(6) and 7.1101(6) Å, while the closest Np−Np distances between adjacent chains are 7.8061(7) and 7.8254(7) Å. Each

dx.doi.org/10.1021/ic202703j | Inorg. Chem. 2012, 51, 3220−3230

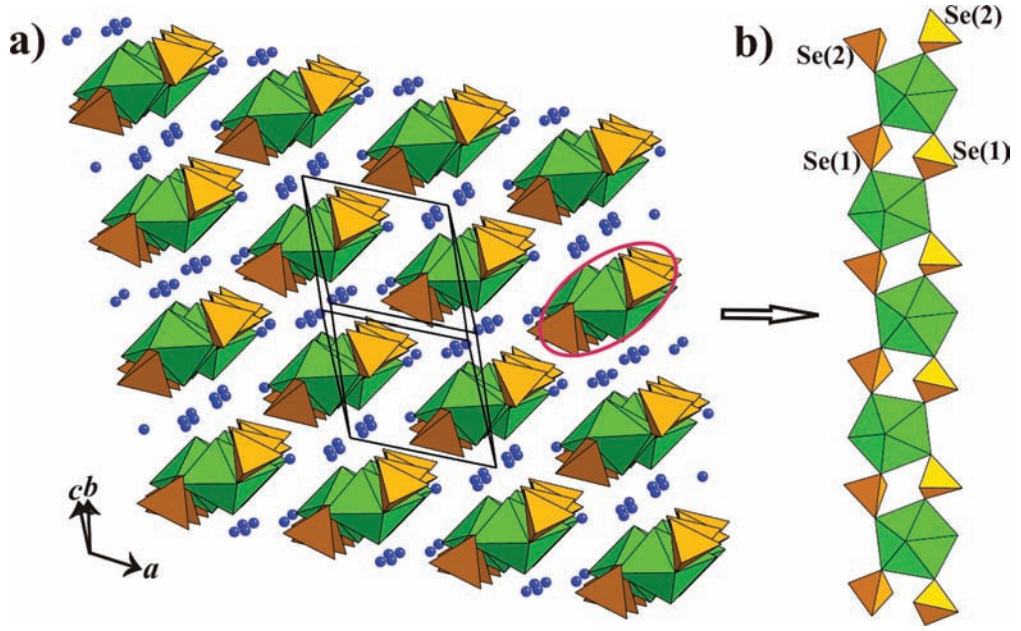

Figure 2. (a) Crystal structure of $Na_3(NpO_2)(SeO_4)_2(H_2O)$ (**2**) with one-dimensional $[(NpO_2)(SeO_4)_2(H_2O)]^{3-}$ chains (circled in red) along the $[0\bar{1}1]$ direction, which are separated by Na^+ cations (blue balls). (b) Depiction of an individual $[(NpO_2)(SeO_4)_2(H_2O)]^{3-}$ chain of corner-sharing green NpO_7 pentagonal bipyramids and orange SeO_4 tetrahedra.

Table 3. Selected Interatomic Distances (Å) and Angles (deg) for $Na_3(NpO_2)(SeO_4)_2(H_2O)$ (2)

Np(1)–O(1)	1.813(3)	Se(1)–O(11)	1.646(3)
Np(1)–O(2)	1.831(3)	Se(2)–O(4)	1.653(3)
Np(1)–O(4)	2.451(3)	Se(2)–O(5)	1.637(3)
Np(1)–O(6)	2.464(3)	Se(2)–O(9)	1.621(3)
Np(1)–O(7)	2.576(3)	Se(2)–O(10)	1.641(3)
Np(1)–O(10)	2.497(3)	Np(1)–Np(1)[a]	6.2541(9)
Np(1)–O(11)	2.445(3)	Np(1)–Np(1)[a]	6.5202(9)
Se(1)–O(3)	1.631(3)	Np(1)–Np(1)[b]	6.3440(9)
Se(1)–O(6)	1.646(3)	Np(1)–Np(1)[b]	6.4090(8)
Se(1)–O(8)	1.634(3)	O(1)–Np(1)–O(2)	176.4(2)

[a]Within a single $[(NpO_2)(SeO_4)_2(H_2O)]^{3-}$ chain. [b]Between adjacent $[(NpO_2)(SeO_4)_2(H_2O)]^{3-}$ chains.

Table 4. Selected Interatomic Distances (Å) and Angles (deg) for $Na_3(NpO_2)(SeO_4)_2(H_2O)_2$ (3)

Np(1)–O(6)	1.838(7)	Se(2)–O(3)	1.62(1)
Np(1)–O(7)	1.815(7)	Se(2)–O(3A)	1.64(1)
Np(1)–O(2) × 2	2.547(5)	Se(2)–O(4)	1.627(9)
Np(1)–O(3)	2.38(1)	Se(2)–O(8)	1.618(7)
Np(1)–O(3A)	2.47(1)	Np(1)–Np(1)[a]	5.9605(6)
Np(1)–O(4)	2.435(9)	Np(1)–Np(1)[a]	7.1101(6)
Se(1)–O(2) × 2	1.658(5)	Np(1)–Np(1)[b]	7.8061(7)
Se(1)–O(5)	1.627(8)	Np(1)–Np(1)[b]	7.8254(7)
Se(1)–O(9)	1.630(7)	O(1)–Np(1)–O(2)	179.8(3)

[a]Within a $[(NpO_2)(SeO_4)_2]^{3-}$ double chain. [b]Between adjacent $[(NpO_2)(SeO_4)_2]^{3-}$ double chains.

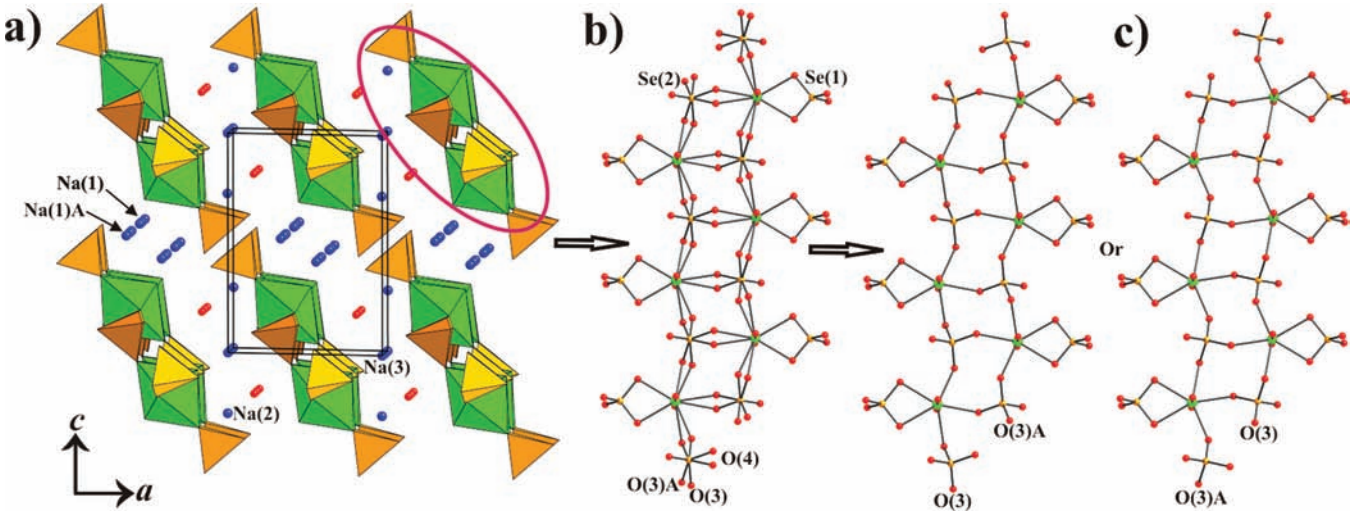

Figure 3. (a) View of the structure of $Na_3(NpO_2)(SeO_4)_2(H_2O)_2$ (**3**) with one-dimensional $[(NpO_2)(SeO_4)_2]^{3-}$ chains (circled in red) along the [010] direction, which are connected by Na^+ cations (blue balls) and H_2O molecules (red balls). (b) Illustration of one $[(NpO_2)(SeO_4)_2]^{3-}$ chain with disordered $Se(2)O_4$ groups. (c) Two configurations of the $[(NpO_2)(SeO_4)_2]^{3-}$ chain.

dx.doi.org/10.1021/ic202703j | Inorg. Chem. 2012, 51, 3220–3230

$Se(1)O_4^{2-}$ anion binds to one NpO_2^+ cation in a bidentate mode, while each $Se(2)O_4^{2-}$ anion binds to three NpO_2^+ cations in a monodentate mode. Se−O distances within the selenate group are in the range of 1.618(7) and 1.658(5) Å. The Na(1) and Na(1A) positions are surrounded by seven O atoms from NpO_2^+ and SeO_4^{2-} ions in total, while $Na(2)^+$ and $Na(3)^+$ cations are coordinated by six O atoms from SeO_4^{2-} and H_2O groups and NpO_2^+, SeO_4^{2-}, and H_2O units, respectively. Na−O distances are in the range of 2.293(8) and 2.81(1) Å. $H_2O(1)$ is bonded to $Na(2)^+$ and $Na(3)^+$ cations.

The structure of **3** is closely related to that of $Na_3(NpO_2)(SO_4)_2(H_2O)_{2.5}$ (**5**), that was prepared by Forbes and Burns.[29] Compound **5** crystallizes in the same space group with comparable unit cell parameters. Its structure consists of $[(NpO_2)(SO_4)_2]^{3-}$ chains with similar connectivities between metal and ligand polyhedra to those in **3**; however, all O atoms from the mondodentate sulfate anions are ordered and there is only one configuration of neptunyl sulfate chains. The Na(3) position in **5**, which corresponds to the disordered Na(1) position in **3**, has large displacement parameters as well, but there is no indication of splitting sites in the refinements of **5**. Instead, Forbes and Burns identified a half occupied water position (site symmetry *m*) which is ∼2.15 Å away from the Na position.[29] The neptunyl sulfate chain found in **5** also exists in the structure of $CaZn_2(NpO_2)_2(SO_4)_4(H_2O)_{10}$ and $[Co(NH_3)_6](NpO_2)(SO_4)_2(H_2O)$.[29,36]

Raman Spectroscopy. Raman spectra in the 400−1050 cm^{-1} region of $Na(NpO_2)(SeO_4)(H_2O)$ (**1**), $Na_3(NpO_2)(SeO_4)_2(H_2O)$ (**2**), and $Na(NpO_2)(SO_4)(H_2O)$ (**4**) are presented in Figure 4. As described in the last section, compounds **1**, **2**, and **4** share certain structural features, which are expected to be reflected in their Raman spectra. Therefore, a preliminary separation of neptunyl(V) vibrational bands from those of the ligands can be achieved by comparing these three spectra. The spectra of **1** and **2** match very well in the region of 400−500 and 840−950 cm^{-1}; the main peaks within the latter region appear as doublets. These bands are attributed to selenate vibrational modes, consistent with the structural studies above, as both structures have two crystallographically unique selenate groups. All of them bond to neptunyl cations in a monodentate manner. The remaining peaks between 650 and 820 cm^{-1} in the selenate, **1**, are comparable to those in its isostructural sulfate analogue, **4**, which appear to originate from the neptunyl vibrations. The Raman bands located at the region of 450−500 and 990−1020 cm^{-1} in **4** are attributed to vibrational modes of sulfate groups.

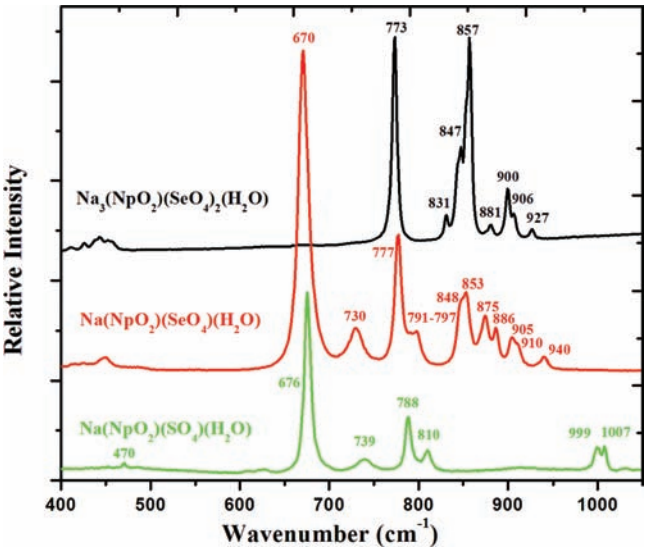

Figure 4. Raman spectra of $Na_3(NpO_2)(SeO_4)_2(H_2O)$ (**2**) (black), $Na(NpO_2)(SeO_4)(H_2O)$ (**1**) (red), and $Na(NpO_2)(SO_4)(H_2O)$[18] (**4**) (green) in the 400−1050 cm^{-1} region (excitation 532 nm).

For linear NpO_2^+ cations in $D_{\infty h}$ symmetry, there are three possible O═Np═O vibrational modes including ν_1 (symmetric stretch, Raman active), ν_2 (bending mode, infrared active), and ν_3 (asymmetric stretch, infrared active). The ν_1 and ν_3 modes of NpO_2^+ units in solutions have been observed at ca. 761 and 824 cm^{-1}, respectively, while the ν_2 band is less certain due to its much lower intensity and potential overlap with ligand modes.[20,37] Tetrahedral TO_4 (T = S, Se) groups (T_d) have four normal modes, ν_1 (symmetric stretch), ν_2 (bending mode), ν_3 (asymmetric stretch), and ν_4 (bending mode). All four vibrations are Raman active with frequencies of 983 (ν_1), 450 (ν_2), 1105 (ν_3), and 611 cm^{-1} (ν_4) for free SO_4^{2-} ions and 833 (ν_1), 335 (ν_2), 875 (ν_3), and 432 cm^{-1} (ν_4) for free SeO_4^{2-} ions in aqueous solutions, respectively.[38] In solid-state compounds, those vibrational modes from both NpO_2^+ and TO_4^{2-} ions are expected to shift and may be split due to their mutual interactions and crystal-field effects. The Raman vibrational bands observed from **1**, **2**, and **4**, together with their peak assignments are summarized in Table 5.

The intense peak at 773 cm^{-1} in the spectrum of **2** can be assigned to the ν_1 of O═Np═O moiety, which is almost the same as the 772 cm^{-1} peak observed for solid $Na_3NpO_2(CO_3)_2{\cdot}nH_2O$. Both compounds lack CCIs.[21] The other two major peaks located at 847 and 857 cm^{-1} are attributed to the ν_1 of two SeO_4 ligands. Vibrational bands observed at 400−500 and 870−950 cm^{-1} are assigned to the ν_4 and ν_3 of SeO_4 groups, respectively. The splits in degenerate vibrations result from the lowering of selenate T_d symmetry caused by their coordination to cations. Because it is close to the values observed for NpO_2^+ cation in solutions,[20,37] the weak band at 831 cm^{-1} is tentatively assigned to the ν_3 mode of the O═Np═O moiety. The appearance in the Raman spectrum of this infrared active asymmetric stretch mode is assigned to the C_s symmetry of $Np(1)O_2^+$ (Table 3) although it can also have contributions from the ν_3 mode of SeO_4 groups. Similar assignments of selenate vibrational modes have been previously reported, e.g. in $Rb_4Be(SeO_4)_2(HSeO_4)_2{\cdot}4H_2O$.[39]

As discussed earlier, **1** and **4** are isostructural and they share similar neptunyl vibrational bands in the region of 600−840 cm^{-1}. Clearly the peaks in the sulfate **4** shift ca. 10 cm^{-1} toward higher frequencies compared to those in the selenate **1**. This behavior agrees well with shorter corresponding $Np-O_{np}$ distances found in **4** (O_{np} = neptunyl oxygen). For example, $Np(1)-O_{np}$ distances are 1.819(4) and 1.845(4) Å in **4** and 1.825(4) and 1.857(4) Å in **1**.[18] There are two crystallographically unique Np sites in the structure of **1** and **4**. Only one of oxo ions within the $Np(1)O_2^+$ unit bonds to the neighboring neptunyl unit, while both of oxo ions within the $Np(2)O_2^+$ unit do. The geometry of the $Np(2)O_2^+$ cation is more closely approximated by $D_{\infty h}$ symmetry, and it has longer $Np-O_{np}$ distances (see Table 2 and ref 16). Therefore, the most intense peak at 670 cm^{-1} for **1** and 676 cm^{-1} for **4** are attributed to the ν_1 of the O═Np(2)═O moiety and the much weaker band at 730 cm^{-1} for **1** and 739 cm^{-1} for **4** are attributed to the ν_1 of the O═Np(1)═O unit. The 760−820

dx.doi.org/10.1021/ic202703j | Inorg. Chem. 2012, 51, 3220−3230

Table 5. Raman Vibrational Frequencies (cm^{-1}) of $Na_3(NpO_2)(SeO_4)_2(H_2O)$ (2), $Na(NpO_2)(SeO_4)(H_2O)$ (1), and $Na(NpO_2)(SO_4)(H_2O)$ (4) in the 400−1050 cm^{-1} region

		$Na_3(NpO_2)(SeO_4)_2(H_2O)$	$Na(NpO_2)(SeO_4)(H_2O)$	$Na(NpO_2)(SO_4)(H_2O)$
O═Np═O	ν_1	773	670 (Np(2)), 730 (Np(1))	676 (Np(2)), 739 (Np(1))
	ν_3	831	777, 791−797	788, 810
SeO_4	ν_1	847, 857	848, 853	
	ν_3	881−927	875−940	
	ν_4	400−500	430−470	
SO_4	ν_1			999, 1007
	ν_2			470

cm^{-1} bands observed in **1** and **4** can be attributed to the ν_3 mode of neptunyl cations, mainly the less symmetrical $Np(1)O_2^+$. A comparable vibrational structure in the region of 720−820 cm^{-1} has been observed in the IR spectrum of $(NpO_2)(NO_3)(CH_3CONH_2)_2$, in which each NpO_2^+ cation coordinates to an adjacent neptunyl unit via CCI.[40] The neptunyl(V) moiety in this nitrate has similar geometry and Np−O_{np} distances (O−Np−O angle 177.6(4)°; distances 1.821(8) and 1.859(8) Å) as the $Np(1)O_2^+$ unit in **1**. However, some of bands in the nitrate were assigned differently, namely 730 cm^{-1} for ρ (CH_3), 756 cm^{-1} (very weak) for ν_1 (NpO_2), 778 and 790 cm^{-1} for ν_3 (NpO_2), and 812 cm^{-1} for ν_2 (NO_3).[40]

The assignments of selenate vibrational bands in **1** are similar to those in **2**. Raman peaks observed in the region of 400−500, 840−860, and 870−950 cm^{-1} are attributed to the ν_4, ν_1, and ν_3 of SeO_4 groups, respectively. In the spectrum of **4**, the ligand vibrational band located at 470 cm^{-1} is attributed to the ν_2 and 999 and 1007 cm^{-1} are attributed to the ν_1 of SO_4 groups.

Magnetism. Representative magnetic susceptibility data from crushed single crystals of $Na(NpO_2)(SeO_4)(H_2O)$ (**1**), obtained over the temperature range of 50−320 K, are shown in Figure 5. The response is attributed to the magnetic

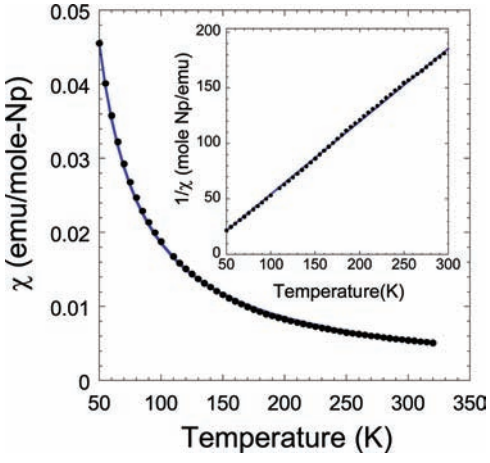

Figure 5. Selected magnetic susceptibility data from 8.2 mg of crushed $Na(NpO_2)(SeO_4)(H_2O)$ (**1**) single crystals (circles) obtained under a constant applied field of 0.05 T. The solid line through the data represents the best fit using the Curie−Weiss law, as discussed in the text. The inset shows the same data, plotted as the inverse susceptibility. The straight-line fit confirms the absence of a measurable temperature-independent contribution to the susceptibility.

moments associated with the $5f^2$ configuration, expected for a Np^{5+} ion. Figure 6 highlights the marked falloff in magnetization as the temperature is increased, interpreted as a low-

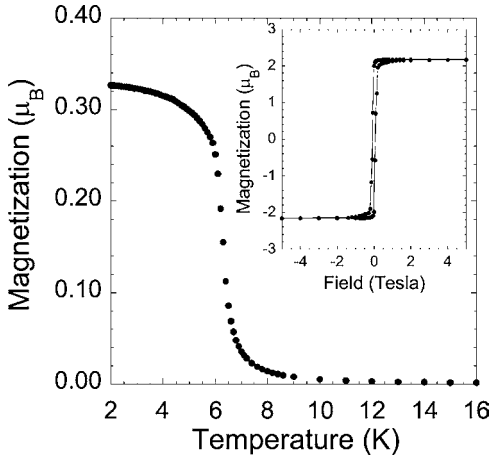

Figure 6. Low temperature magnetization for $Na(NpO_2)(SeO_4)(H_2O)$ (**1**), measured under an applied field of 0.005 T highlights the sudden onset of spontaneous magnetization at 6.5(2) K. The field dependence, shown in the inset, reveals the near-absence of a hysteresis, indicative of a soft ferromagnet.

temperature ferromagnetic ordering of the Np moments, with an onset temperature of 6.5(2) K. The field response of the magnetization at 2 K, shown as an inset of Figure 6, exhibits saturation behavior at low field, a result supporting the interpretation of ferromagnetic−moment coupling at low temperatures. Similar magnetic behavior was recently reported for $(NpO_2)_2(SeO_4)(H_2O)_4$, which has a related 2D neptunyl(V) CCI network. The tetrahydrate structure is more complex, with four crystallographically independent Np positions contributing to the measured response.[12] The tetrahydrate ferromagnetically orders at 8(1) K.

The saturation value of the magnetization, μ_{SAT}, represented by the high-field limit of the magnetization, is related to the ground state wave function:

$$\mu_{SAT} = -gJ\mu_B$$

where J represents the total angular momentum within the Russell−Saunders coupling formalism. The experimentally determined magnetization extrapolates to 2.2 (1) μ_B per Np, at high fields, significantly smaller than the 3.2 μ_B free-ion saturation moment expected for a f^2 configuration with a $^3H_4$ ground multiplet but similar to the 1.98(8) μ_B previously reported for $(NpO_2)_2(SeO_4)(H_2O)_4$.[12] Crystal-field splitting could reduce the moment observed here because of the strong axial symmetry imparted to the Np ion by the oxo moieties.[41,42] This effect requires the replacement of J states with wave functions Γ_n that include the appropriate mixing of $|m_J\rangle$ states. Crystal-field effects have been previously shown to account for similar reductions in the Pr^{3+} saturation moments in oxide

dx.doi.org/10.1021/ic202703j | Inorg. Chem. 2012, 51, 3220−3230

systems. Pr^{3+}, which also has a f^2 configuration, has reported saturation moments ranging from negligible to about 2 μ_B or larger.[42,43] An alternate but related explanation for the reduced saturation could arise if the ordering involves a canted-spin orientation that partially cancels the measured moment. This interpretation is not favored when comparing the results here with those previously reported for $(NpO_2)_2(SeO_4)(H_2O)_4$, which has four inequivalent Np and a more complicated structure. Further single crystal studies are required to sort out these ambiguities. Also similar to the behavior of $(NpO_2)_2(SeO_4)(H_2O)_4$ is the persistence of magnetic correlations to temperatures well above the loss of long-range order suggested by the susceptibility data. This observation has been previously reported for other layered materials in which in-plane coupling is stronger than any out-of-plane interactions, the latter of which may include competitive coupling forces.[44,45] The difference in Np−Np in-ribbon distances, about 4.1−4.2 Å, to the out-of-ribbon shortest Np−Np interactions of 6.0 to 6.5 Å supports this interpretation.

Well above the temperature at which the moments appear to be ordered, the magnetic response of $Na(NpO_2)(SeO_4)(H_2O)$ (**1**) behaves like a classic paramagnet, as described by the modified Curie−Weiss Law:

$$\chi_{exp} = \frac{C}{T - \theta} + \chi_{TIP}$$

in which θ, the Weiss constant, is an indication of the an interaction energy between local spins, expressed as a temperature, and χ_{TIP} is the temperature-independent paramagnetism (TIP). C is the Curie constant and is related to the effective magnetic moment by

$$\mu_{eff} = \left(\frac{3kC}{N\mu_B{}^2}\right)^{1/2}$$

with k as the Boltzmann constant, N as Avogadro's number, and μ_B the Bohr magneton unit, equal to 0.927×10^{-20} erg/Gauss. A plot of χ^{-1} vs T, shown as an inset to Figure 5 over the temperature range of 50−320 K, is a straight line, indicating that the TIP contribution is negligible and hence is not included in the fit.

Fitting the data directly to the Curie−Weiss Law yields an average Np effective moment of $\mu_{eff} = 3.65(10)$ μ_B and a Weiss constant of $\theta = 14(1)$ K. The effective moment is within error of the full free-ion moment of 3.58 μ_B expected for an f^2 system using the Russell−Saunders coupling scheme, and the Weiss constant is small and positive, consistent with the interpretation of ferromagnetic spin ordering at 6.5(2) K.

DISCUSSION

While exploring the neptunyl(V) selenate chemistry, we have synthesized and characterized six compounds including previously reported $(NpO_2)_2(SeO_4)(H_2O)_n$ (n = 1, 2, 4) and the titled three Na-contained phases.[12] $(NpO_2)_2(SeO_4)(H_2O)_2$, $(NpO_2)_2(SeO_4)(H_2O)_4$, and **1** are isostructural with their sulfate analogues, whereas $(NpO_2)_2(SeO_4)(H_2O)$ and **3** are structurally close to the sulfates. Reported as a neptunyl (V) selenate, **2** shares the same structural feature as the uranyl(VI) sulfates. Within this small database the structural chemistry of neptunyl sulfates generally is very similar to that of the selenates, not surprising considering the similar ligand geometries. The discrepancy in the actinyl−sulfate and −selenate interactions, observed in both solid-state structures and aqueous solutions, may arise in part from the different proton affinities and sizes of anions. For example, high energy X-ray scattering (HEXS) studies on UO_2^{2+}−sulfate and −selenate ion pairs in aqueous solutions suggested that uranyl to sulfate-ion orientation appears rigid and uranyl selenate ion pairs appear to rotate freely.[15−17] This behavior may help to explain the rotational disordering of the selenate group in **3**, while the sulfate group in **5** is ordered. In fact, there are more reported examples of actinyl compounds with disordered selenate anions, such as α-$Mg_2(UO_2)_3(SeO_4)_5(H_2O)_{16}$ and $M_2(UO_2)_3(SeO_4)_5(H_2O)_{16}$ (M = Co, Zn).[46,47] Sulfate anions generally bind to actinyl cations in both monodentate and bidentate modes, while selenate ligands connect to actinyl units predominantly in a monodentate mode.[14] This can be understood from the steric repulsion between the center atoms in the ligand and actinyl groups. The larger Se atom affects more steric repulsion in the closer packed bidentate mode. Compound **3** is one of only a few examples of a bidentate selenate group coordinating to an actinyl cation.[14] Furthermore, the sulfate and selenate ligands display slightly different complexing ability to the actinyl cations.[48,49] Studies of ligand effects on uranyl(VI) vibrational spectra indicated that the stability of these complexes increases as the stretching frequencies decrease.[50,51] In the present study, the NpO_2^+ cations in the selenate, **1** have longer Np−O_{np} distances exhibiting lower stretching frequency than those in the isostructural sulfate, **4**. Np−O_{np} distances in $(NpO_2)_2(SeO_4)(H_2O)_n$ (n = 2, 4) are longer than those in corresponding sulfates as well.[12,31,52] Taken together, these results show the selenate forming stronger connections with neptunyl(V) cations in the solid than the sulfate, thus leading to weaker Np−O_{np} bonds in the selenates. This hypothesis can be further tested by measuring the vibrational spectra of isostructural solid-state neptunyl(V) sulfates and selenates and the stability constants of these complexes in solutions.

The structures of $(NpO_2)_2(SeO_4)(H_2O)_n$ contain a three-dimensional CCI network of neptunyl pentagonal bipyramids for the monohydrate and two-dimensional CCI neptunyl layers for the dihydrate and the tetrahydrate, respectively.[12] The inclusion of Na^+ cations in the titled compounds affords a mechanism to interrupt the neptunyl lattice connectivity by providing additional bonding to the neptunyl oxygen ion. As a result, compound **1** with a Na:Np ratio of 1:1 adopts a structure with CCI ribbons of neptunyl pentagonal bipyramids, while neptunyl pentagonal bipyramids in compound **2** and **3** with Na:Np ratios of 3:1 do not have direct interactions but instead are bridged by selenate tetrahedra. Similar correlations of the CCI network connectivity with the presence of other cations has been observed.[9] As discussed in the previous work, CCIs occur in every inorganic neptunyl(V) phase that include no additional cations to the best of our knowledge.[9] These observations suggest that the neptunyl(V) oxo groups tend to form CCIs with neighboring AnO_2^+ units to fulfill their bonding requirements in the absence of sufficient other cations. The lattice dimensionalities of the overall structures in these six selenates decrease with the number of Na^+ cations and hydrates and consequently become less condensed, as reflected in relative densities of Np in each structure (0.01057 Np/Å^3 for monohydrate, 0.009702 Np/Å^3 for dihydrate, and 0.007391 Np/Å^3 for tetrahydrate, 0.006389 Np/Å^3 for **1**, 0.004027 for Np/Å^3 for **2**, and 0.003248 Np/Å^3 for **3**).[12]

dx.doi.org/10.1021/ic202703j | Inorg. Chem. 2012, 51, 3220−3230

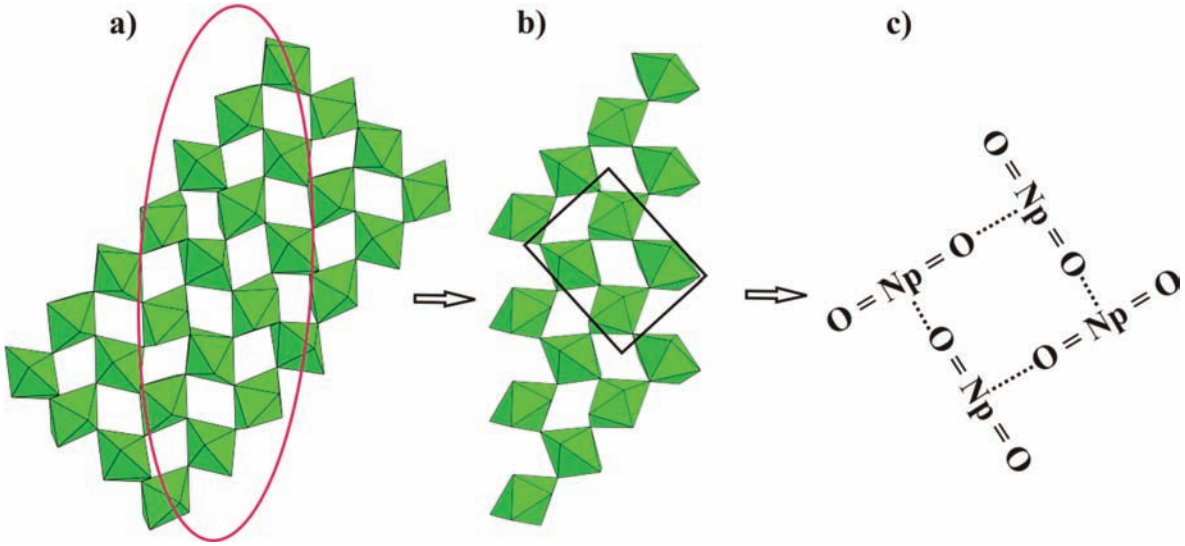

Figure 7. (a) Two-dimensional square net of neptunyl(V) pentagonal bipyramids bonded through cation−cation interactions. (b) Neptunyl ribbon found in $Na(NpO_2)(SeO_4)(H_2O)$ (**1**) can be considered as a four-Np wide strip of the "cationic square net". (c) Illustration of an individual neptunyl square.

Compounds **2** and **3** have similar formulas, differing only in the number of waters of hydration. Both structures are constructed from one-dimensional neptunyl selenate chains. However, the connectivities between neptunyl cations and ligands are substantially different within these chains. In compound **2**, each NpO_2^+ cation is coordinated by four monodentate SeO_4^{2-} anions and one H_2O molecule, while the NpO_2^+ cation in **3** is coordinated by one bidentate SeO_4^{2-} and three monodentate SeO_4^{2-} anions in the equatorial plane. In other words, for compound **2**, each SeO_4^{2-} group bridges two NpO_2^+ units in a monodentate mode and each H_2O coordinates to one NpO_2^+ unit; However, in the case of **3**, one of the SeO_4^{2-} groups coordinates to one NpO_2^+ unit in a bidentate mode and the other one connects to three neptunyl cations in a monodentate mode, and H_2O molecules only bind to Na^+ cations.

The Raman spectra of **1**, **2**, and **4** complement well the existing vibrational data (mostly IR) on solid-state neptunyl(V) compounds, especially those containing CCIs.[10,21,40,53,54] Assignments of neptunyl(V) stretching modes can be highly uncertain, complicated by potential overlap with ligand bands (e.g., ν_3 for NpO_2 vs ν_1 for SeO_4), the presence of multiple Np sites, and distortions of the linear neptunyl moiety. Depending upon the number and the character of CCI bonds, the symmetry and Np−O_{np} distances can change substantially, splitting degenerate modes and shifting stretching bands. In the present study, we selectively measured the Raman spectra of three phases, within which **1** and **2** adopt similar monodentate selenate ligands and **1** and **4** are isostructural with equivalent neptunyl units. With the use of these comparative structures, the vibrational bands attributed to the netpunyl moiety and ligands can be separated unambiguously, with the exception of the 831 cm^{-1} band in the spectrum of **2**. One of the distinctive features in these three spectra is the significant shifts of the neptunyl stretching bands due to the CCIs. For example, the ν_1 mode of the O=Np=O moiety located at 773 cm^{-1} for **2** (no CCIs, Np−O_{np} distances: 1.813(3) and 1.831(3) Å), 730 cm^{-1} for Np(1) in **1** (one CCI, Np−O_{np} distances: 1.825(4) and 1.857(4) Å), 670 cm^{-1} for Np(2) in **1** (two CCIs, Np−O_{np} distances: 1.840(4) and 1.854(4) Å). The other important feature is the presence of multiple degenerate ν_3 bands of NpO_2^+, as displayed in the spectrum of **1**. Complicated by the lack of published precedent, the assignments of ν_3 bands to individual Np sites require further studies. Additional systematic measurements of Raman and IR spectra of neptunyl(V) compounds with CCIs are required to build a more quantitatively and metrical understanding of the correlation between symmetry and Np−O_{np} distances and their stretching modes.

We have recently reported trends associated with magnetic properties of neptunyl(V) compounds and their CCI networks.[12] One important observation is that all six ferromagnetic compounds including $(NpO_2)(O_2CH)(H_2O)$,[55] $[(NpO_2)_2(O_2C)_2C_6H_4(H_2O)_3]\cdot H_2O$,[56] β-$Ag(NpO_2)(SeO_3)$,[57] $(NpO_2)_2(SeO_4)(H_2O)_4$,[12] $NaK_3(NpO_2)_4(SO_4)_4(H_2O)_2$,[18] and **4**[18] adopt an arrangement of NpO_2^+ cations into squares through CCIs (Figure 7). More specifically, the first four phases consist of two-dimensional neptunyl "cationic square nets" (Figure 7a), while the last two contain four-Np wide strips of these cationic square nets (Figure 7b). The organization of NpO_2^+ cations into a square lattice through CCIs (Figure 7c) appears to promote ferromagnetic interactions between Np(V) centers. These compounds exhibit ordering temperatures ranging from 4.5 to 12.3 K, and their saturation moments are all significantly smaller than the full moment expected from an f^2 system. Compound **1** is isostructural with **4**, adopting ribbons of cationic square nets as well (Figure 7b). The magnetic results of **1** fit well into this class of behavior with an ordering temperature of 6.5(2) K and a saturation moment of 2.2(1) μ_B. The difference in the fractal lattice dimensionalities based on NpO_2^+ CCI interactions for these seven ferromagnetic compounds does not appear to significantly impact their magnetic properties, which are very similar.

■ CONCLUSIONS

To further explore the neptunyl(V) selenate system, three new sodium contained hydrates: $Na(NpO_2)(SeO_4)(H_2O)$ (**1**), $Na_3(NpO_2)(SeO_4)_2(H_2O)$ (**2**), and $Na_3(NpO_2)(SeO_4)_2(H_2O)_2$ (**3**) have been synthesized from aqueous solutions and structurally characterized. Compound **1** is

dx.doi.org/10.1021/ic202703j | Inorg. Chem. 2012, 51, 3220−3230

isostructural with its sulfate analogue, whereas the structures of **2** and **3** are closely related to corresponding sulfates. These results are consistent with the fact that sulfate and selenate ligands have same charges and similar tetrahedral geometries. However a discrepancy in the neptunl(V)−sulfate and −selenate interactions has been observed in the structures of **3** and $Na_3(NpO_2)(SO_4)_2(H_2O)_{2.5}$ (**5**). The monodentate selenate group in **3** is disordered in two orientations, while the corresponding sulfate group is ordered in **5**. The selenate ligand appears to form slightly stronger complexes with neptunyl(V) cations than the sulfate. Compared to two- or three-dimensional CCI networks of neptunyl(V) found in $(NpO_2)_2(SeO_4)(H_2O)_n$ (n = 1, 2, 4), inclusion of Na^+ cations disrupts the neptunyl lattice in titled compounds, as the structure of **1** contains CCI NpO_2^+ ribbons whereas the structures of **2** and **3** are constructed from one-dimensional neptunyl selenate chains without CCIs. As indicated from structural studies showing two crystallographically unique Np sites both involving CCIs in isostructural **2** and **4** and only one Np position without CCIs in **2**, Raman spectra of **1** and $Na(NpO_2)(SeO_4)(H_2O)$ (**4**) are comparable in the region of neptunyl stretching modes and they are more complex than those in **2**. For **1** and **4**, the symmetric stretch modes of neptunyl unit shift significantly toward lower frequencies than that in **2**, and there are several asymmetric stretch bands. Compound **1** exhibits evidence for ferromagnetic ordering at 6.5(2) K, which is consistent with magnetic behaviors of **4** and other neptunyl(V) compounds with similar arrangements of NpO_2^+ in CCI squares.

■ ASSOCIATED CONTENT

Ⓢ Supporting Information

Crystallographic files in cif format for $Na(NpO_2)(SeO_4)(H_2O)$ (**1**), $Na_3(NpO_2)(SeO_4)_2(H_2O)$ (**2**), and $Na_3(NpO_2)(SeO_4)_2(H_2O)_2$ (**3**). This material is available free of charge via the Internet at http://pubs.acs.org or by contacting FIZ Karlsruhe at +497247808 666 (fax) or crysdata@fiz-karlsruhe.de (e-mail) on quoting the depository numbers CSD-423925 (H2 Na Np O7 Se), CSD-423926 (H2 Na3 Np O11 Se2), and CSD-423927 (H4 Na3 Np O12 Se2). Selected Na−O Distances (Å) for $Na(NpO_2)(SeO_4)(H_2O)$ (**1**), $Na_3(NpO_2)(SeO_4)_2(H_2O)$ (**2**), and $Na_3(NpO_2)(SeO_4)_2(H_2O)_2$ (**3**) are listed in Tables S1, S2, and S3 respectively.

■ AUTHOR INFORMATION

Corresponding Author

*E-mail: gjin@anl.gov. Phone: +1 630 252 3658.

Notes

The authors declare no competing financial interest.

■ ACKNOWLEDGMENTS

This work was performed at Argonne National Laboratory, operated by UChicagoArgonne LLC for the United States Department of Energy, under contract number DE-AC02-06CH11357 and was supported by DOE Office of Basic Energy Sciences, Chemical Sciences, Heavy Elements Chemistry.

■ REFERENCES

(1) Konings, R. J. M.; Morss, L. R.; Fuger, J., Thermodynamic Properties of Actinides and Actinide Compounds. In *The Chemistry of the Actinide and Transactinide Elements*; 3rd ed.; Morss, L. R., Edelstein, N. M., Fuger, J., Katz, J. J., Eds.; Springer: Dordrecht, 2006; Vol. 4, p 2113−2224.

(2) Burns, P. C. *Can. Mineral* **2005**, *43*, 1839−1894.

(3) Yoshida, Z.; Johnson, S. G.; Kimura, T.; Krsul, J. R., Neptunium. In *The Chemistry of the Actinide and Transactinide Elements*; 3rd ed.; Morss, L. R., Edelstein, N. M., Fuger, J., Katz, J. J., Eds.; Springer: Dordrecht, 2006; Vol. 2, p 699−812.

(4) Antonio, M. R.; Soderholm, L.; Williams, C. W.; Blaudeau, J. P.; Bursten, B. E. *Radiochim. Acta* **2001**, *89*, 17−25.

(5) Forbes, T. Z.; Wallace, C.; Burns, P. C. *Can. Mineral.* **2008**, *46*, 1623−1645.

(6) Krot, N. N.; Grigoriev, M. S. *Russ. Chem. Rev.* **2004**, *73*, 89−100.

(7) Sullivan, J. C.; Hindman, J. C.; Zielen, A. J. *J. Am. Chem. Soc.* **1961**, *83*, 3373−3378.

(8) Forbes, T. Z.; Burns, P. C.; Skanthakumar, S.; Soderholm, L. *J. Am. Chem. Soc.* **2007**, *129*, 2760−2761.

(9) Jin, G. B.; Skanthakumar, S.; Soderholm, L. *Inorg. Chem.* **2011**, *50*, 6297−6303.

(10) Grigorev, M. S.; Yanovskii, A. I.; Struchkov, Y. T.; Bessonov, A. A.; Afonaseva, T. V.; Krot, N. N. *Sov. Radiochem.* **1989**, *31*, 397−403.

(11) Charushnikova, I. A.; Krot, N. N.; Starikova, Z. A. *Radiochemistry* **2000**, *42*, 439−445.

(12) Jin, G. B.; Skanthakumar, S.; Soderholm, L. *Inorg. Chem.* **2011**, *50*, 5203−5214.

(13) Almond, P. M.; Skanthakumar, S.; Soderholm, L.; Burns, P. C. *Chem. Mater.* **2007**, *19*, 280−285.

(14) Krivovichev, S. V.; Burns, P. C., Actinide Compounds Containing Hexavalent Cations of the VI Group Elements (S, Se, Mo, Cr, W). In *Structural Chemistry of Inorganic Actinide Compounds*; Krivovichev, S. V., Burns, P. C., Tananaev, I. G., Eds.; Elsevier: Amsterdam, 2007; p 95−182.

(15) Neuefeind, J.; Skanthakumar, S.; Soderholm, L. *Inorg. Chem.* **2004**, *43*, 2422−2426.

(16) Soderholm, L.; Skanthakumar, S.; Neuefeind, J. *Anal. Bioanal. Chem.* **2005**, *383*, 48−55.

(17) Skanthakumar, S.; Soderholm, L. Unpublished results.

(18) Forbes, T. Z.; Burns, P. C.; Soderholm, L.; Skanthakumar, S. *Chem. Mater.* **2006**, *18*, 1643−1649.

(19) Basile, L. J.; Sullivan, J. C.; Ferraro, J. R.; LaBonville, P. *Appl. Spectrosc.* **1974**, *28*, 142−145.

(20) Guillaume, B.; Begun, G. M.; Hahn, R. L. *Inorg. Chem.* **1982**, *21*, 1159−1166.

(21) Madic, C.; Hobart, D. E.; Begun, G. M. *Inorg. Chem.* **1983**, *22*, 1494−1503.

(22) Kalman, A.; Cruickshank, D. W. J. *Acta Crystallogr. Sect. B* **1970**, *26*, 436.

(23) Bruker. *APEX2 Version 2009.5-1 and SAINT Version 7.34a Data Collection and Processing Software*; Bruker Analytical X-Ray Instruments, Inc.: Madison, WI, USA, 2009.

(24) Bruker. *SMART Version 5.054 Data Collection and SAINT-Plus Version 6.45a Data Processing Software for the SMART System*; Bruker Analytical X-Ray Instruments, Inc.: Madison, WI, USA, 2003.

(25) Sheldrick, G. M. *Acta Crystallogr., Sect. A* **2008**, *64*, 112−122.

(26) Gelato, L. M.; Parthe, E. *J. Appl. Crystallogr.* **1987**, *20*, 139−143.

(27) Boudreaux, E. A.; Mulay, L. N. *Theory and Applications of Molecular Paramagnetism*; Wiley Interscience: New York, 1976.

(28) FournierJ. M.Struct. Bonding (Berlin)1985

(29) Forbes, T. Z.; Burns, P. C. *J. Solid State Chem.* **2005**, *178*, 3445−3452.

(30) Charushnikova, I. A.; Krot, N. N.; Polyakova, I. N. *Crystallogr. Rep.* **2006**, *51*, 201−204.

(31) Forbes, T. Z.; Burns, P. C. *J. Solid State Chem.* **2009**, *182*, 43−48.

(32) Tabachenko, V. V.; Serezhkin, V. N.; Serezhkina, L. B.; Kovba, L. M. *Koord. Khim.* **1979**, *5*, 1563−1568.

(33) Krivovichev, S. V.; Kahlenberg, V. *Z. Naturfor. Sec. B* **2005**, *60*, 538−542.

(34) Mercier, R.; Thi, M. P.; Colomban, P. *Solid State Ionics* **1985**, *15*, 113−126.

(35) Gesing, T. M.; Ruscher, C. H. *Z. Anorg. Allg. Chem.* **2000**, *626*, 1414−1420.

(36) Grigorev, M. S.; Fedoseev, A. M.; Budantseva, N. A.; Yanovskii, A. I.; Struchkov, Y. T.; Krot, N. N. *Radiokhimiya* **1990**, *33*, 54−61.
(37) Jones, L. H.; Penneman, R. A. *J. Chem. Phys.* **1953**, *21*, 542−544544.
(38) Nakamoto, K. Application in Inorganic Chemistry. In *Infrared and Raman Spectra of Inorganic and Coordination Compounds*; 5th ed.; John Wiley & Sons, Inc.: New York, 1997; Sect. II, p 153−320.
(39) Georgiev, M.; Wildner, M.; Marinova, D.; Stoilova, D. *Solid State Sci.* **2010**, *12*, 899−905.
(40) Andreev, G. B.; Budantseva, N. A.; Antipin, M. Y.; Krot, N. N. *Russ. J. Coord. Chem.* **2002**, *28*, 434−438.
(41) Wybourne, B. G. *Spectrosopic properties of rare earths*; Interscience: New York, 1965.
(42) Staub, U.; Soderholm, L. Electronic 4f state splittings in cuprates. In *Handbook on the Physics and Chemistry of Rare Earths*. Gschneidner Jr, K. A., Eyring, L., Maple, M. B., Eds.; Elsevier Science BV: New York, 2000; Vol. *30*, p 491−545.
(43) Lea, K. R.; L., J. M.; Wolf, W. P. *J. Phys. Chem. Solids* **1962**, *23*, 1281−1405.
(44) Mason, T. E. Neutron scattering studies of spin flucstuations in high-temperature superconductors. In *Handbook on the Physics and Chemistry of Rare Earths*; Gschneidner, K. A. J., Eyring, L., Maple, M. B., Eds.; Elsevier Science: New York, 2001; Vol. *31*, p 281−314.
(45) Lynn, J. W.; Skanthakumar, S. Neutron scattering studies of spin flucstuations in high-temperature superconductors. In *Handbook on the Physics and Chemistry of Rare Earths*; Gschneidner, K. A. J., Eyring, L., Maple, M. B., Eds.; Elsevier Science: New York, 2001; Vol. *31*, p 315−350.
(46) Krivovichev, S. V.; Kahlenberg, V. *Z. Anorg. Allg. Chem.* **2004**, *630*, 2736−2742.
(47) Krivovichev, S. V.; Kahlenberg, V. *J. Alloys Compd.* **2005**, *395*, 41−47.
(48) Grenthe, I.; Fuger, J.; Konings, R. J. M.; Lemire, R. J.; Muller, A. B.; Nguen-Trung, C.; Wanner, H. In *Chemical Thermodynamics of Uranium*; North-Holland Elsevier Science Publishers B.V.: Amsterdam, 1992.
(49) Sladkov, V. *ELECTROPHORESIS* **2010**, *31*, 3482−3491.
(50) McGlynn, S. P.; Smith, J. K.; Neely, W. C. *J. Chem. Phys.* **1961**, *35*, 105−116.
(51) Nguyen Trung, C.; Begun, G. M.; Palmer, D. A. *Inorg. Chem.* **1992**, *31*, 5280−5287.
(52) Grigoriev, M. S.; Ianovskii, A. I.; Fedoseev, A. M.; Budantseva, N. A.; Struchkov, I. T.; Krot, N. N.; Spitsyn, V. I. *Doklady Akademii Nauk Sssr* **1988**, *300*, 618−622.
(53) Grigorev, M. S.; Baturin, N. A.; Budantseva, N. A.; Fedoseev, A. M. *Radiochemistry* **1993**, *35*, 151−156.
(54) Budantseva, N. A.; Fedoseev, A. M.; Grigorev, M. S.; Potemkina, T. I.; Afonaseva, T. V.; Krot, N. N. *Sov. Radiochem.* **1988**, *30*, 578−581.
(55) Nakamoto, T.; Nakada, M.; Nakamura, A.; Haga, Y.; Onuki, Y. *Solid State Commun.* **1999**, *109*, 77−81.
(56) Nakamoto, T.; Nakada, M.; Nakamura, A. *J. Nucl. Sci. Technol.* **2002**, No. Suppl. 3, 102−105.
(57) Jobiliong, E.; Oshima, Y.; Brooks, J. S.; Albrecht-Schmitt, T. E. *Solid State Commun.* **2004**, *132*, 337−342.